Title: Predictive factors for the development of peritumoral brain edema after LINAC-based radiation treatment in patients with intracranial meningioma

Short title: Peritumoral brain edema after radiation

Authors: Ryang-Hun Lee[1], Jae Min Kim[1], Jin Hwan Cheong[1], Je Il Ryu[1], Young Soo Kim[2], Myung-Hoon Han[1]*

[1]Department of Neurosurgery, Hanyang University Guri Hospital, 153 Gyeongchun-ro, Guri 471-701, Gyonggi-do, Korea, Tel.:+82.31-560-2326, Fax: +82.31-560-2327

[2]Department of Neurosurgery, Hanyang University Medical Center, 222-1, Wangsimni-ro, Seongdong-gu, Seoul, Korea 133-792, Tel.: +82-2-2290-8500, Fax: +82-2-2281-0954

***Corresponding author:** Myung-Hoon Han, M.D., Ph.D.

Department of Neurosurgery, Hanyang University Guri Hospital, 153 Gyeongchun-ro, Guri 471-701, Gyonggi-do, Korea

Tel.: +82.31-560-2328

Fax: +82.31-560-2327

E-mail: gksmh80@gmail.com

ORCID ID: 0000-0003-1728-5017

Competing Interests: The authors have declared that no competing interests exist.

Abstract

Background and purpose: Disruption of the tumor-brain barrier in meningioma plays a critical role in the development of peritumoral brain edema (PTBE). We hypothesized that osteoporotic conditions may be associated with PTBE occurrence after radiation in patients with intracranial meningioma.

Methods: We measured Hounsfield units (HU) of the frontal skull on simulation brain CT in patients who underwent linear accelerator (LINAC)-based radiation treatment for intracranial meningioma. Receiver operating characteristic curve analysis was performed to determine the optimal cut-off values for several predictive factors. The cumulative hazard for PTBE was estimated and classified according to these factors. Hazard ratios were then estimated to identify independent predictive factors associated with the development of PTBE after radiation in intracranial meningioma patients.

Results: A total of 83 intracranial meningiomas in 76 patients who received LINAC-based radiation treatment in our hospital over an approximate 5-year period were included for the study. We found mean frontal skull HU ≤630.625 and gross tumor volume >7.194 cc to be independent predictors of PTBE after radiation treatment in patients with meningioma (hazard ratio, 8.38; P=0.021; hazard ratio, 5.78; P=0.034, respectively). In addition, patients who were ≥65 years showed a marginally significant association with PTBE.

Conclusions: Our study suggests that possible osteoporotic conditions, large tumor volume, and older age may be associated with PTBE occurrence after LINAC-based radiation treatment for intracranial meningioma. In the future we anticipate that these findings may enhance the understanding of the underlying mechanisms of PTBE after radiation in

meningioma patients.

Introduction

Meningiomas are the most common extra-axial primary intracranial benign tumors and account for 13–26% of all primary intracranial tumors [1]. Although microsurgical tumor resection is the treatment of choice for symptomatic meningiomas, gross total resection of meningiomas is not always possible due to various conditions such as tumor size, location, adjacent neurovascular structures, or the patient's medical status. Radiation therapy is used as a treatment for meningiomas when the remnant tumor is present after surgery or when surgical resection is not an option [2]. Radiotherapy for meningioma is accepted as a safe treatment modality. Approximately 5% to 40% of patients experience treatment-related complications [3]. It was reported that symptomatic brain edema occurs in 37.5% of patients with parasagittal meningiomas after gamma knife radiosurgery [4].

Disruption of the tumor-brain barrier in meningioma plays a critical role in the development of peritumoral brain edema (PTBE) [5]. A previous study regarding microscopic anatomy of the brain–meningioma interface reported the presence of arachnoid trabeculae at the brain–meningioma contact interface [6]. We previously demonstrated a close correlation between bone mineral density (BMD) and Hounsfield unit (HU) values [7]. In addition, we suggested that systemic osteoporosis is negatively associated with the integrity of arachnoid trabeculae as both the bone and the arachnoid trabeculae are composed of type 1 collagen [7,8]. We hypothesized that osteoporotic conditions may be associated with PTBE after radiation in intracranial meningioma patients.

To test this hypothesis, we measured HU values in the frontal bone from simulation brain computed tomography (CT) of patients who underwent linear accelerator (LINAC)-based

radiation treatment for intracranial meningioma in our hospital. We evaluated other predictive risk factors for PTBE in meningioma after radiation treatment.

Methods

Study patients

This study was approved by the Institutional Review Board of Hanyang University Medical Center, Korea, and conformed to the tenets of the Declaration of Helsinki. Owing to the retrospective nature of the study, the need for informed consent was waived. All patient records were anonymized prior to analysis.

We retrospectively extracted data for all consecutive patients who were diagnosed with intracranial meningioma and received LINAC-based radiation treatment for the first time from the database of our hospital's NOVALIS registry, from July 7, 2014 to July 31, 2019. The registry has been designed for prospective research since July 7, 2014. Demographic patient information, prescribed radiation dose, and fractionation data were extracted from the NOVALIS registry.

All intracranial meningiomas were diagnosed by radiologic findings or histological confirmation following resection. All radiologic findings were confirmed by experienced neuro-radiologists. We only included patients with meningioma who underwent at least one follow-up imaging (CT/magnetic resonance imaging [MRI]) after LINAC-based radiation treatment in order to assess the occurrence of PTBE. The last imaging follow-up period after treatment was investigated in all study patients. PTBE was defined as the radiological confirmation of newly developed PTBE or the progression of preexisting PTBE after radiation treatment with newly developed neurological deficits. All patients had no preexisting PTBE among the patients who did not underwent surgery for meningioma before radiation treatment. Two patients were excluded due to no measurable cancellous bone of the frontal skull on brain

CT.

Radiation technique

All patients were treated using the NOVALIS Tx system (Varian Medical Systems, CA, USA; Brainlab, Feldkirchen, Germany) in our hospital. A noninvasive thermoplastic mask was used to perform simulation-computed tomography (CT) for radiation treatment. The Novalis ExacTrac image system and robotic couch of the NOVALIS Tx system allowed us to adjust the patients' positions according to the information from the real-time image acquisition. Patients were treated with a 6 MV LINAC-based radiation treatment within 1 week from the day when the CT simulation was performed.

Gross tumor volume (GTV) was defined as the contrast-enhanced area on T1-weighted MRI images. In surgery patients, the GTV was defined as the postoperative resection cavity and the area of residual tumor in cases of subtotal resection. The clinical target volume (CTV) was identical to the GTV. The planning target volume (PTV) was defined as a symmetrical 0 to 2-mm expansion from the CTV. In case the tumor was located near an organ at risk, we adjusted the PTV with no expansion in the area of the tumor that was close to the organ at risk. The iPlan (Brainlab, Feldkirchen, Germany) and Eclipse (Varian, CA, USA) that are 3D treatment/planning systems of the NOVALIS Tx, were used for radiation planning using MRI/CT-fusion images in all intracranial meningioma patients. The 3D treatment/planning system automatically calculated the GTV, CTV, and PTV in all treated patients. We attempted to achieve tight conformality of the treatment isodose to the 3D reconstructed meningioma geometry.

Stereotactic radiosurgery (SRS) was defined as a single session treatment, hypofractionated

SRS (hf-SRS) as 2 to 5 fractions, hypofractionated stereotactic radiotherapy (hFSRT) as 6 to 10 fractions, and fractionated stereotactic radiotherapy (FSRT) as doses delivered in >10 sessions (1.8–2.0 Gy/fraction) [9,10]. The biologically equivalent dose (BED) for the tumor was calculated according to the following equation: BED = nd × (1 + d/10), where n is the number of fractions, d is the dose per fraction, and α/β=10.

Measurement of frontal skull HU

Simulation-CT images (Philips Brilliance Big Bore CT Simulators) for radiation planning were used to measure the frontal skull HU values in all study patients. A previous study reported that variations in HU values across five CT scanners were in the range of 0–20 HU [11]. We previously demonstrated detailed methods for measuring HU values at each of four lines on the frontal cancellous bone. This was between the right and left coronal sutures on axial CT slices at the point where the lateral ventricles disappear [7,12]. The HU value of the frontal cancellous bone was measured using the "Linear histogram graph" function in the picture archiving and communication system (PACS). The PACS automatically calculated the maximum, minimum, and mean HU values according to the values on the drawn line. We recorded the mean HU value on each line of cancellous bone at the frontal bone region (Fig. 1).

Figure 1. Measurement of HU values at each of four lines on the frontal bone
The PACS automatically calculated the maximum, minimum, and mean HU values according to the values on the drawn line. The mean HU value on each of the four lines was recorded. (A) Right lateral; (B) right medial; (C) left medial; (D) left lateral. HU=Hounsfield unit;

PACS=picture archiving and communication system.

To avoid including cortical bone, all brain CT images were magnified for HU measurement. All frontal skull HU measurements were conducted by a trained neurosurgeon blinded to the clinical data of all patients.

Other study variables

Clinical data including height, weight, hypertension, and diabetes were extracted from electronic medical records. Body mass index (BMI) was calculated as weight/ (height × height) and expressed in kg/m^2. Tumor location was confirmed by neuro-radiologists using the PACS.

Statistical methods

Continuous variables were expressed as mean ± SD or median with an interquartile range (IQR) and categorical variables were expressed as counts and percentage. The chi-square test and Student's t-test were used to assess statistical differences between non-PTBE and PTBE groups. The mean frontal skull HU value ([mean right lateral HU + mean right medial HU + mean left medial HU + mean left lateral HU]/4) was used in all analyses.

Receiver operating characteristic (ROC) curve analysis was performed to determine the optimal cut-off values of several factors for predicting PTBE after radiation treatment in meningioma patients. The optimal cut-off value was defined as the shortest distance from the upper left corner. The distance between each point on the ROC curve and the upper left corner was calculated as $\sqrt{(1-\text{sensitivity})^2+(1-\text{specificity})^2}$ [13].

The cumulative hazard for PTBE was estimated using Kaplan-Meier analysis classified according to several predictive factors, with censoring of patients who had no PTBE on the last brain CT/MRI. Hazard ratios (HRs) with 95% confidence intervals (CIs) were then calculated using univariate and multivariate Cox regression analysis. This was used to identify independent predictive factors associated with the development of PTBE after LINAC-based radiation treatment in intracranial meningioma patients. The *P*-values less than 0.05 were considered statistically significant.

All statistical analyses were performed using R version 3.5.2 (https://www.r-project.org/).

Results

Characteristics of study patients

Seventy-Six patients with 83 intracranial meningiomas who received LINAC-based radiation treatments in our hospital over an approximate 5-year period were enrolled in the study. The mean patient age was 62.8 years and 80.7% of patients were female. The median imaging follow-up period was 456 days and 45.8% of patients had surgical resection before radiation treatment. The mean GTV and BED were 8.4 cc and 48.8 Gy, respectively. Non-PTBE and PTBE patients demonstrated significant differences in age. Details of patient characteristics are presented in Table 1.

Table 1. Characteristics of patients with intracranial meningioma who underwent LINAC-based radiation treatment in our hospital

Characteristics	PTBE (-)	PTBE (+)	Total	*P*
Number (%)	70 (84.3)	13 (15.7)	83 (100)	
Sex, female, n (%)	56 (80.0)	11 (84.6)	67 (80.7)	1.000
Age, mean ± SD, y	61.4 ± 11.6	70.2 ± 9.0	62.8 ± 11.7	0.012
Imaging follow-up period, median (IQR), days	477.0 (194.8–788.0)	435.0 (198.5–1062.5)	456.0 (198.0–862.0)	0.251
BMI, mean ± SD, kg/m^2	24.7 ± 3.7	24.2 ± 3.2	24.6 ± 3.6	0.675
Height, mean ± SD, cm	159.1 ± 9.4	155.9 ± 7.8	158.6 ± 9.2	0.247

Weight, mean ± SD, kg	62.5 ± 11.5	58.5 ± 6.7	61.9 ± 10.9	0.228
Prior surgical resection, n (%)	35 (50.0)	3 (23.1)	38 (45.8)	0.128
Pathology, n (%)				0.317
WHO grade I	24 (34.3)	2 (15.4)	26 (31.3)	
WHO grade II	8 (11.4)	0	8 (9.6)	
WHO grade III	3 (4.3)	1 (7.7)	4 (4.8)	
GTV, mean ± SD, cc	7.6 ± 9.9	12.4 ± 9.8	8.4 ± 10.0	0.116
PTV, mean ± SD, cc	11.7 ± 13.7	17.6 ± 11.1	12.7 ± 13.4	0.153
Location, n (%)				0.733
Convexity	22 (31.4)	5 (38.5)	27 (32.5)	
Parasagittal or parafalcine	14 (20.0)	4 (30.8)	18 (21.7)	
Sphenoid ridge	7 (10.0)	1 (7.7)	8 (9.6)	
Cerebellopontine angle	7 (10.0)	2 (15.4)	9 (10.8)	
Posterior fossa	7 (10.0)	1 (7.7)	8 (9.6)	
Parasellar or petroclival	10 (14.3)	0	10 (12.0)	
Other	3 (4.3)	0	3 (3.6)	
Marginal radiation dose, mean ± SD, Gy	31.5 ± 12.0	26.7 ± 5.6	30.8 ± 11.4	0.161
Fractionation, n (%)				0.372
SRS	13 (18.6)	3 (23.1)	16 (19.3)	
hf-SRS (2-5 fractions)	39 (55.7)	9 (69.2)	48 (57.8)	

hFSRT (6-10 fractions)	4 (5.7)	1 (7.7)	5 (6.0)	
FSRT	14 (20.0)	0	14 (16.9)	
Dose per fraction median (IQR), Gy	5.8 (4.8–7.0)	6.0 (5.4–11.3)	5.8 (5.3–7.0)	0.418
BED (α/β = 10), mean ± SD, Gy	49.2 ± 8.7	46.4 ± 4.7	48.8 ± 8.2	0.264
BED (α/β = 10), median (IQR), Gy	46.8 (44.5–52.7)	45.8 (41.6–49.2)	45.9 (43.7–51.2)	0.264
Past medical history, n (%)				
Hypertension	29 (41.4)	6 (46.2)	35 (42.2)	0.768
Diabetes	13 (18.6)	3 (23.1)	16 (19.3)	0.708

LINAC, linear accelerator; PTBE, peritumoral brain edema; SD, standard deviation; IQR, interquartile range; BMI, body mass index; WHO, world health organization; GTV, gross tumor volume; PTV, planning target volume; SRS, stereotactic radiosurgery; hf-SRS, hypofractionated stereotactic radiosurgery; hFSRT, hypofractionated stereotactic radiotherapy; FSRT, fractionated stereotactic radiotherapy; BED, biologically equivalent dose

Mean frontal skull HU values, according to PTBE in study patients

Table 2 shows descriptive statistics of frontal skull HU values according to PTBE after radiation treatment.

Table 2. Descriptive statistics of the mean frontal skull HU values according to peritumoral

257 brain edema after LINAC-based radiation treatment in patients with intracranial meningi
258 oma

Characteristics	PTBE (-)	PTBE (+)	Total	*P*
Overall mean frontal skull HU value, median (IQR)	733.6 (559.3–870.1)	547.8 (415.6–677.5)	725.8 (527.0–853.3)	0.018
Overall mean frontal skull HU value, mean ± SD	735.4 ± 246.2	564.4 ± 161.7	708.6 ± 242.4	0.018
Mean HU value at each of four sites in the frontal skull, mean ± SD				
Right lateral	707.3 ± 245.1	579.2 ± 124.9	687.2 ± 234.6	0.070
Right medial	773.6 ± 268.7	588.9 ± 191.3	744.7 ± 265.9	0.021
Left medial	738.8 ± 271.4	566.2 ± 201.9	711.8 ± 268.2	0.032
Left lateral	722.1 ± 259.0	523.2 ± 166.3	690.9 ± 256.5	0.009
Average, medial	756.2 ± 266.0	577.5 ± 190.6	728.2 ± 262.9	0.024
Average, lateral	714.7 ± 247.9	551.2 ± 143.3	689.1 ± 241.4	0.024
Classification of skull HU, n (%)				0.005
Mean frontal skull HU ≤630.6	23 (32.9)	10 (76.9)	33 (39.8)	
Mean frontal skull HU >630.6	47 (67.1)	3 (23.1)	50 (60.2)	

259 HU, Hounsfield unit; LINAC, linear accelerator; PTBE, peritumoral brain edema; IQR,
260 interquartile range; SD, standard deviation

261

262

We observed significant differences in values of the mean frontal skull HU and classification of the skull HU between non-PTBE and PTBE groups. The overall average mean frontal skull HU value was 725.8 in all study patients, 733.6 in the non-PTBE group and 547.8 in the PTBE group.

Determination of the optimal cut-off values of predictive factors for PTBE after radiation

The optimal cut-off values of age, mean frontal skull HU, and GTV for the prediction of PTBE in patients with intracranial meningioma after radiation were 65 years (area under the curve [AUC]=0.730; sensitivity=84.6%; specificity=65.7%; *P*=0.009), 630.625 (AUC=0.716; sensitivity=76.9%; specificity=67.1%; *P*=0.014), and 7.194 cc (AUC=0.706; sensitivity=69.2%; specificity=71.4%; *P*=0.019), respectively (Fig. 2A–C).

Figure 2. Comparisons of age mean frontal skull HU value, GTV, and BED between PTBE and non-PTBE groups This includes the determination of the optimal cut-off values of the predictive factors for PTBE occurrence after radiation in intracranial meningioma. (A) Boxplots with dot plots of age according to the PTBE and ROC curve to identify the optimal cutoff value of age for the prediction of PTBE; (B) Boxplots with dot plots of mean frontal skull HU according to the PTBE and ROC curve to identify the optimal cutoff value of mean frontal skull HU for the prediction of PTBE; (C) Boxplots with dot plots of GTV according to the PTBE and ROC curve to identify the optimal cutoff value of GTV for the prediction of PTBE; (D) Boxplots with dot plots of BED according to the PTBE and ROC curve to identify

the optimal cutoff value of BED for the prediction of PTBE. PTBE=peritumoral brain edema; AUC=area under the curve; HU=Hounsfield unit; GTV=gross tumor volume; BED= biologically equivalent dose; ROC=receiver operating characteristic.

However, BED did not show statistical significance in the ROC analysis (P=0.335), (Fig. 2D).

According to the cut-off values, the study patients were classified into (1) ≥65 years (2) mean frontal skull HU ≤630.625, and (3) GTV >7.194 cc groups.

Cumulative hazard of PTBE after radiation according to several predictive factors

The incidence of PTBE was significantly higher among patients who were ≥65 years, with a mean frontal skull HU ≤630.625, and a GTV >7.194 cc in the clinical course of intracranial meningioma after LINAC-based radiation treatment (Fig. 3A–C).

Figure 3. Cumulative hazard of PTBE after LINAC-based radiation treatment for intracranial meningioma according to the several predictive factors

(A) age group (cut-off value of 65); (B) mean frontal skull HU (cut-off value of 630.625); (C) GTV (cut-off value of 7.194); (D) two fractionation categories (SRS or hf-SRS versus hFSRT or FSRT). PTBE=peritumoral brain edema; HU=Hounsfield unit; GTV=gross tumor volume; SRS=stereotactic radiosurgery; hf-SRS= hypofractionated stereotactic radiosurgery; hFSRT= hypofractionated stereotactic radiotherapy; FSRT= fractionated stereotactic radiotherapy.

Patients with ≤5 fractionation (SRS or hf-SRS) also tended to have higher rates of PTBE after radiation (Fig. 3D, *P*=0.159).

Independent predictive factors for PTBE after radiation in meningioma patients

The multivariate Cox regression analysis identified a mean frontal skull HU ≤630.625 and GTV >7.194 cc as independent predictors of PTBE after LINAC-based radiation treatment in intracranial meningioma patients (HR, 8.38; 95% CI, 1.38–50.73; *P*=0.021; HR, 5.78; 95% CI, 1.14–29.39; *P*=0.034, respectively); (Table 3).

Table 3. Univariate and multivariate Cox regression analyses for the development of peritumoral brain edema in patients with intracranial meningioma after LINAC-based radiation treatment based on predictive variables

	Univariate analysis		Multivariate analysis	
Variable	HR (95% CI)	*P*	HR (95% CI)	*P*
Sex				
Male	Reference		Reference	
Female	1.27 (0.28–5.80)	0.759	0.83 (0.16–4.16)	0.818
Age group				
<65 years	Reference		Reference	
≥65 years	11.24 (2.47–51.27)	0.002	5.20 (1.00–27.13)	0.050

BMI (per 1 BMI increase)	0.95 (0.80–1.14)	0.610	0.98 (0.77–1.26)	0.893
Mean frontal skull HU				
≤630.6	9.83 (2.13–45.23)	0.003	8.38 (1.38–50.73)	0.021
>630.6	Reference		Reference	
GTV				
≤7.2 cc	Reference		Reference	
>7.2 cc	4.17 (1.27–13.74)	0.019	5.78 (1.14–29.39)	0.034
Location				
Convexity	2.41 (0.74–7.88)	0.145	1.96 (0.53–7.23)	0.310
Other regions	Reference		Reference	
BED (α/β=10) (per 1 Gy increase)	0.96 (0.89–1.04)	0.352	0.97 (0.85–1.11)	0.688
Fractionation (per 1 fraction increase)	0.92 (0.82–1.04)	0.184	0.77 (0.49–1.20)	0.240

HR, hazard ratio; CI, confidence interval; BMI, body mass index; HU, Hounsfield unit; GTV, gross tumor volume; BED, biologically equivalent dose

Patients who were ≥65 years showed a marginal statistically significant association with PTBE occurrence after full adjustment (HR, 5.20; 95% CI, 1.00–27.13; *P*=0.050).

Although we adjusted the age group in the multivariate analysis, a negative relationship between age and BMD may affect our results. We also identified a close association between age and mean frontal skull HU values in the study patients in S1 Fig. We further performed additional multivariate Cox regression with the adjustment for age as a continuous variable in the S1 Table. The results showed that the mean frontal skull HU ≤630.625 was maintained as an independent predictor of PTBE (HR, 6.99; 95% CI, 1.12–43.60; *P*=0.037). When we

337 adjusted for the past medical history, mean frontal skull HU ≤630.625 showed a strong
338 association with PTBE in the study patients (S2 Table).

339 When the patients were divided into the risk factor group (age ≥65 years and skull HU
340 ≤630.625 and GTV >7.194 cc) and others, the rate of PTBE was significantly higher in the risk
341 factor group than in the others (Fig. 4). The univariate Cox analysis showed a strong significant
342 association between PTBE and the risk factor group (HR, 21.92; 95% CI, 6.10 to 78.74;
343 $P<0.001$).

344
345
346
347
348
349
350
351
352
353
354
355
356
357
358
359
360
361

Discussion

We found that PTBE was independently associated with possible low BMD and large tumor volume in the clinical course of intracranial meningioma after LINAC-based radiation treatment. Older age showed a marginal independent association with PTBE occurrence after radiation. The possible low BMD group (mean skull HU ≤630.6) had an approximate 7.0 to 9.0-fold increased risk of PTBE after adjusting for other predictive factors including age. To our knowledge, this study is the first to suggest that BMD is associated with PTBE after radiation treatment in patients with intracranial meningioma.

It is well accepted that the tumor-brain barrier disruption may be an essential component of PTBE formation [5]. Glioblastoma and metastatic tumors usually induce PTBE. However, in contrast to glioblastomas and metastases, meningiomas are encapsulated and are separated from the underlying normal cerebral cortex by the arachnoid membrane and pia mater. The arachnoid membrane is impermeable to fluids due to its' tight intercellular junctions [14]. It is thought that the arachnoid membrane may act as a mechanical and biochemical buffer against mediators released from a meningioma [15]. It is probable that the arachnoid membrane blocks the spread of edema-associated proteins such as endothelial growth factor/vascular permeability factor and vasogenic edema fluids from meningiomas from the peritumoral brain tissue [3]. A previous study that examined the microscopic anatomy of the brain-meningioma interface, also reported that the degree of arachnoid disruption correlated with the presence of perifocal edema [6].

Interestingly, a microscopic examination of the brain-meningioma interface revealed proliferation of hyperplastic arachnoid trabeculae, (below the arachnoid membrane at the

brain–meningioma interface) in the meningioma with a thin connective capsule (shown in Fig. 1A of the study) [6]. After the study, it was reported that the arachnoid trabeculae and granulations are composed of type 1 collagen [16]. The arachnoid is composed of two layers. An outer part of the arachnoid is the arachnoid barrier layer and is an actual membrane cover. An inner part is the arachnoid trabeculae maintaining the stability of the subarachnoid space and cerebrospinal fluid flow to support the arachnoid barrier layer [17]. Arachnoid cap cells are believed to be of meningioma cell origin [18]. Therefore, it is possible to postulate that meningioma from arachnoid cap cells may naturally push the arachnoid trabeculae into the pia mater [19]. As the tumor grows, it could also be assumed that arachnoid trabeculae may be sandwiched between the pia mater and meningioma. This may form part of the tumor-brain contact interface. Compression due to the growth of a tumor on adjacent venous structures, leptomeninges, and the cerebral cortex may lead to an increase in hydrostatic pressure [20].

It is well documented that type 1 collagen is a major component of bone. Osteoporosis is a systemic disease that affects systemic bone mass and microarchitecture throughout the body. We previously reported the close association between mean frontal skull HU and BMD [7,12]. We also demonstrated that systemic osteoporosis may negatively affect the integrity of arachnoid trabeculae and granulations because bone, arachnoid trabeculae, and granulations are all composed of type 1 collagen [7,8]. Supporting our hypothesis, osteogenesis imperfecta, that is caused by mutations in type 1 procollagen genes (*COL1A1/COL1A2*), is associated with communicating hydrocephalus [21]. We believe that trabeculae, which are sandwiched between the pia mater and meningioma, may be more impaired and weakened in osteoporotic patients when compared to healthy patients.

Previous studies described that irradiation affects collagen structure and can lead to collagen changes and damage [22,23]. When the meningioma is not treated with surgery or radiation

409 therapy, tumor growth is the primary cause of damage to the tumor-brain contact interface
410 including the arachnoid trabeculae. After radiation, this contact interface may be damaged by
411 radiation activities [3].

412 Based on the above findings and assumptions, we propose the following hypothetical
413 mechanism as an explanation for the association between possible low BMD, large tumor
414 volume, and PTBE after radiation for intracranial meningioma. As tumor grows, the tumor may
415 push more of the arachnoid trabeculae into the pia mater and cause damage to the tumor-brain
416 contact interface. The larger the tumor, the greater the likelihood of damage to the tumor-brain
417 contact interface including the arachnoid trabeculae. The damage to the arachnoid trabeculae
418 due to compression by the tumor will be more severe in osteoporotic patients. Radiation may
419 aggravate the damaged tumor-brain contact interface including the arachnoid trabeculae and
420 may lead to tumor-brain barrier disruption. We hypothesized that the more damaged the
421 arachnoid trabeculae are at the tumor-brain interface due to low BMD and large tumor volume,
422 the higher the possibility will be of tumor-brain barrier disruption after radiation therapy.
423 Tumor-brain barrier disruption may result in PTBE formation in meningioma patients after
424 radiation.

425 Loosening of the microstructure network and the volume reduction of aging white matter
426 may increase the possibility of PTBE. This allows direct transmission of edematous fluids into
427 the white matter [24]. We believe that thorough precautions are required with older patients
428 with osteoporosis and large tumor volume, after radiation therapy for intracranial meningioma.
429 We also found that BED was not associated with PTBE occurrence in our study. We propose
430 that this was because we did not use extremely high radiation doses and the narrow BED range
431 may not have resulted in significant differences in PTBE occurrence [3]. We believe that the
432 status of the brain-meningioma contact interface, including the arachnoid trabeculae, is a more

433 important factor than the radiation dosage in predicting PTBE occurrence after radiation for
434 meningioma. Although it falls short of significance, multi-fraction seems to be important for
435 prevention of PTBE after radiation for meningioma.

436 Our study has several limitations. First, due to the retrospective nature of the study, the
437 length of follow-ups and the number of follow-up images varied widely. Second, HU
438 measurement errors may have occurred. However, all brain CT images were magnified for HU
439 measurement to reduce errors. We excluded patients with no measurable cancellous bone of
440 the frontal skull in the simulation brain CT. To reduce measurement errors, we estimated mean
441 HU values in four areas of the frontal skull and averaged them. Third, although HU values are
442 correlated with BMD, HU values may not reflect the exact BMD values. Fourth, heterogeneity
443 in tumor location and absence of histological confirmation in many cases may affect the results
444 of the study. Lastly, the small number of cases may have reduced the statistical power and
445 validation.

446 In conclusion, our study suggests that possible osteoporotic conditions, large tumor volume,
447 and older age may be associated with PTBE occurrence after LINAC-based radiation treatment
448 for intracranial meningioma. We believe that these findings may be helpful for predicting
449 PTBE occurrence during the clinical course of meningioma after radiation. In the future, we
450 anticipate that the findings of this study may enhance the understanding of the underlying
451 mechanisms of PTBE after radiation in meningioma patients.

452

453

454

455

456

Author Contributions:

Dr M.H.H had full access to all data in the study and takes responsibility for the integrity of the data and the accuracy of the data analysis. All authors reviewed the manuscript.

Ryang-Hun Lee-

Data curation

Investigation

Writing – original draft

Jae Min Kim-

Supervision

Jin Hwan Cheong-

Supervision

Resources

Je Il Ryu-

Supervision

Writing – review & editing

Young Soo Kim-

Supervision

480

481 Myung-Hoon Han-

482 Conceptualization

483 Methodology

484 Formal Analysis

485 Visualization

486 Writing – original draft

487

488

489

490

491

492

493

494

495

496

497

498

Acknowledgments: This study was funded by Basic Science Research Program through the National Research Foundation of Korea (NRF) funded by the Ministry of Science, ICT & Future Planning (NRF-2019R1G1A1085289).

References

1. Whittle IR, Smith C, Navoo P, Collie D. Meningiomas. The Lancet. 2004;363: 1535–1543. doi:10.1016/S0140-6736(04)16153-9

2. Pinzi V, Bisogno I, Prada F, Ciusani E, Fariselli L. Radiotherapy of meningioma: a treatment in need of radiobiological research. International Journal of Radiation Biology. 2018;94: 621–627. doi:10.1080/09553002.2018.1478157

3. Cai R, Barnett GH, Novak E, Chao ST, Suh JH. Principal risk of peritumoral edema after stereotactic radiosurgery for intracranial meningioma is tumor-brain contact interface area. Neurosurgery. 2010;66: 513–522. doi:10.1227/01.NEU.0000365366.53337.88

4. Singh VP, Kansai S, Vaishya S, Julka PK, Mehta VS. Early complications following gamma knife radiosurgery for intracranial meningiomas. J Neurosurg. 2000;93 Suppl 3: 57–61. doi:10.3171/jns.2000.93.supplement

5. Hou J, Kshettry VR, Selman WR, Bambakidis NC. Peritumoral brain edema in intracranial meningiomas: the emergence of vascular endothelial growth factor-directed therapy. Neurosurg Focus. 2013;35: E2. doi:10.3171/2013.8.FOCUS13301

6. Nakasu S, Fukami T, Jito J, Matsuda M. Microscopic anatomy of the brain-meningioma interface. Brain Tumor Pathol. 2005;22: 53–57. doi:10.1007/s10014-005-0187-0

7. Han M-H, Won YD, Na MK, Kim CH, Kim JM, Ryu JI, et al. Association Between Possible Osteoporosis and Shunt-Dependent Hydrocephalus After Subarachnoid

554 Hemorrhage. Stroke. 2018;49: 1850–1858. doi:10.1161/STROKEAHA.118.021063

555 8. Bae I-S, Kim JM, Cheong JH, Ryu JI, Han M-H. Association between bone mineral
556 density and brain parenchymal atrophy and ventricular enlargement in healthy individuals.
557 Aging (Albany NY). 2019;11: 8217–8238. doi:10.18632/aging.102316

558 9. Meniai-Merzouki F, Bernier-Chastagner V, Geffrelot J, Tresch E, Lacornerie T, Coche-
559 Dequeant B, et al. Hypofractionated Stereotactic Radiotherapy for Patients with
560 Intracranial Meningiomas: impact of radiotherapy regimen on local control. Sci Rep.
561 2018;8: 13666. doi:10.1038/s41598-018-32124-8

562 10. Kirkpatrick JP, Soltys SG, Lo SS, Beal K, Shrieve DC, Brown PD. The radiosurgery
563 fractionation quandary: single fraction or hypofractionation? Neuro-oncology. 2017;19:
564 ii38–ii49. doi:10.1093/neuonc/now301

565 11. Birnbaum BA, Hindman N, Lee J, Babb JS. Multi-detector row CT attenuation
566 measurements: assessment of intra- and interscanner variability with an anthropomorphic
567 body CT phantom. Radiology. 2007;242: 109–119. doi:10.1148/radiol.2421052066

568 12. Na MK, Won YD, Kim CH, Kim JM, Cheong JH, Ryu JI, et al. Opportunistic osteoporosis
569 screening via the measurement of frontal skull Hounsfield units derived from brain
570 computed tomography images. PLoS ONE. 2018;13: e0197336.
571 doi:10.1371/journal.pone.0197336

572 13. Tuan NT, Adair LS, He K, Popkin BM. Optimal cutoff values for overweight: using body
573 mass index to predict incidence of hypertension in 18–65-year-old Chinese adults. J Nutr.
574 2008;138: 1377–1382.

14. Weller RO. Microscopic morphology and histology of the human meninges. Morphologie. 2005;89: 22–34.

15. Conti A, Pontoriero A, Siddi F, Iatì G, Cardali S, Angileri FF, et al. Post-Treatment Edema after Meningioma Radiosurgery is a Predictable Complication. Cureus. 8. doi:10.7759/cureus.605

16. Saboori P, Sadegh A. Histology and Morphology of the Brain Subarachnoid Trabeculae. Anat Res Int. 2015;2015: 279814. doi:10.1155/2015/279814

17. Yamashima T. Human Meninges: Anatomy and Its Role in Meningioma Pathogenesis. In: Lee JH, editor. Meningiomas. London: Springer; 2009. pp. 15–24. doi:10.1007/978-1-84628-784-8_3

18. Wiemels J, Wrensch M, Claus EB. Epidemiology and etiology of meningioma. J Neurooncol. 2010;99: 307–314. doi:10.1007/s11060-010-0386-3

19. arachnoid_cap_cell [Operative Neurosurgery]. [cited 25 Oct 2019]. Available: https://operativeneurosurgery.com/doku.php?id=arachnoid_cap_cell

20. Hanna A, Boggs DH, Kwok Y, Simard M, Regine WF, Mehta M. What predicts early volumetric edema increase following stereotactic radiosurgery for brain metastases? J Neurooncol. 2016;127: 303–311. doi:10.1007/s11060-015-2034-4

21. Charnas LR, Marini JC. Communicating hydrocephalus, basilar invagination, and other neurologic features in osteogenesis imperfecta. Neurology. 1993;43: 2603–2608. doi:10.1212/wnl.43.12.2603

595 22. Miller JP, Borde BH, Bordeleau F, Zanotelli MR, LaValley DJ, Parker DJ, et al. Clinical
596 doses of radiation reduce collagen matrix stiffness. APL Bioengineering. 2018;2: 031901.
597 doi:10.1063/1.5018327

598 23. Maslennikova A, Kochueva M, Ignatieva N, Vitkin A, Zakharkina O, Kamensky V, et al.
599 Effects of gamma irradiation on collagen damage and remodeling. Int J Radiat Biol.
600 2015;91: 240–247. doi:10.3109/09553002.2014.969848

601 24. Gunning-Dixon FM, Brickman AM, Cheng JC, Alexopoulos GS. Aging of cerebral white
602 matter: a review of MRI findings. Int J Geriatr Psychiatry. 2009;24: 109–117.
603 doi:10.1002/gps.2087

604

605

606

607

608

609

610

611

612

Supporting Information

S1 Figure. Scatterplot with linear regression line showing the association between age and mean frontal skull HU values. HU=Hounsfield unit.

S1 Table. Uni- and multivariate Cox regression analyses for the development of peritumoral brain edema in patients with intracranial meningioma after LINAC-based radiation treatment based on predictive variables (adjusted for age as continuous variable).

S2 Table. Uni- and multivariate Cox regression analyses for the development of peritumoral brain edema in patients with intracranial meningioma after LINAC-based radiation treatment based on predictive variables (adjusted for age as continuous variable and past medical history).

A

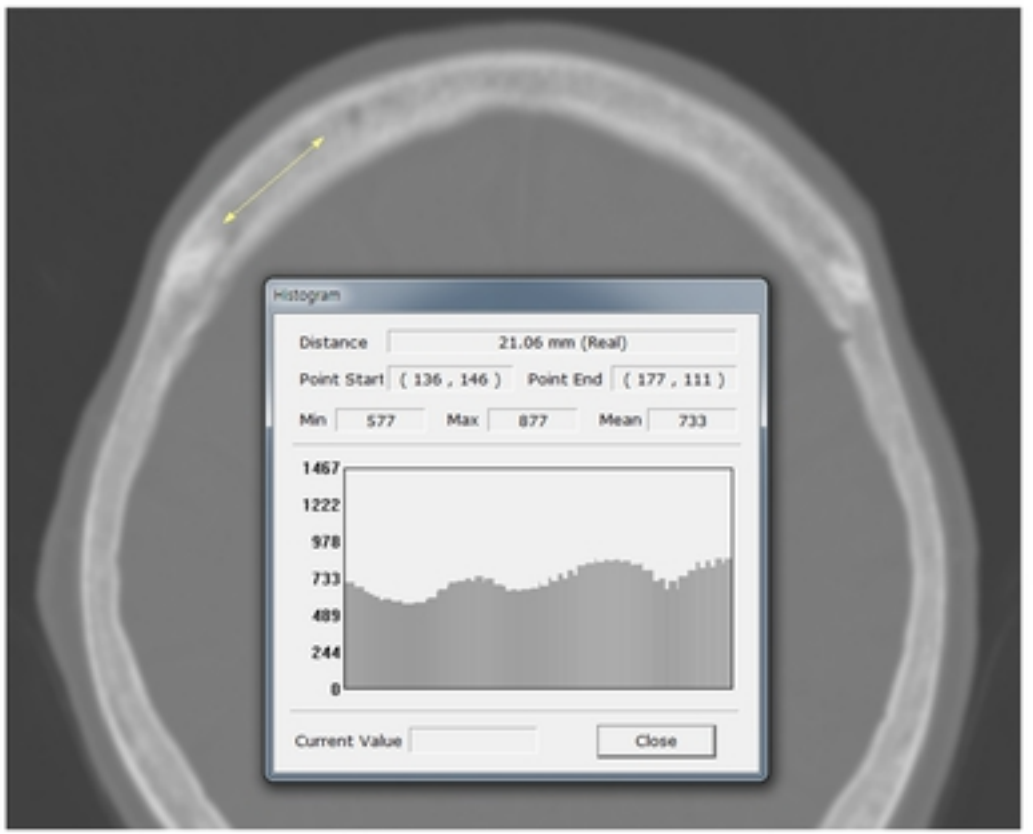

B

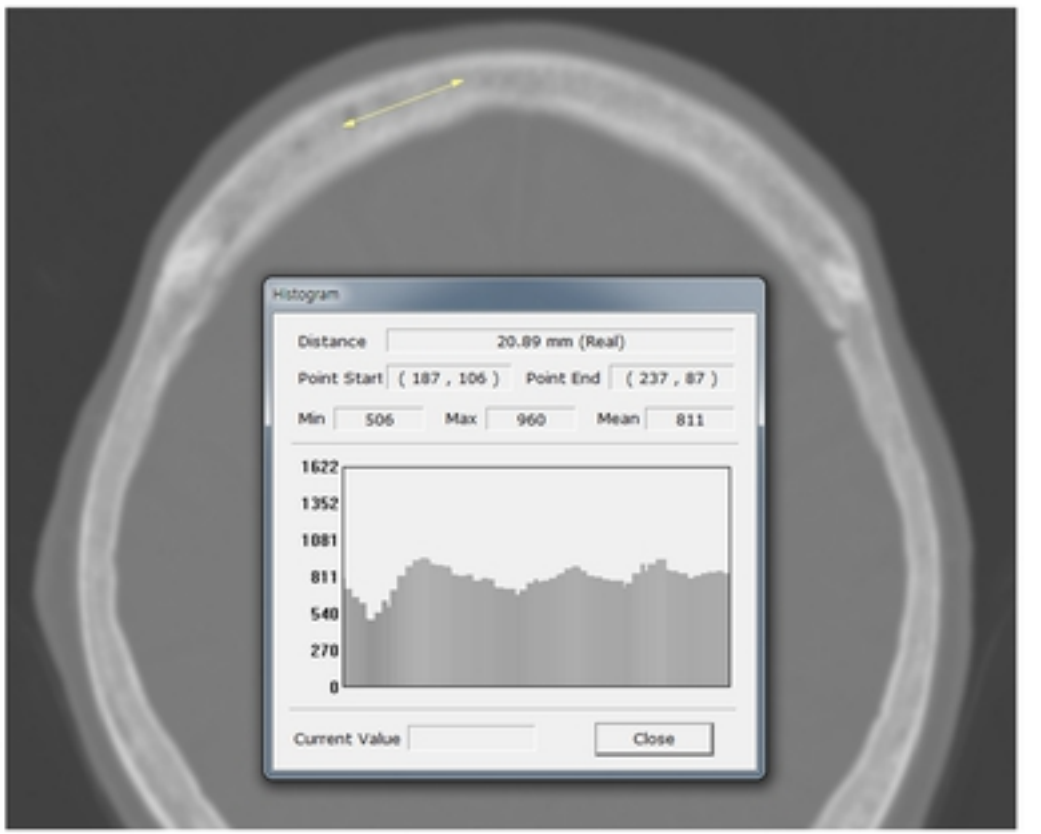

C

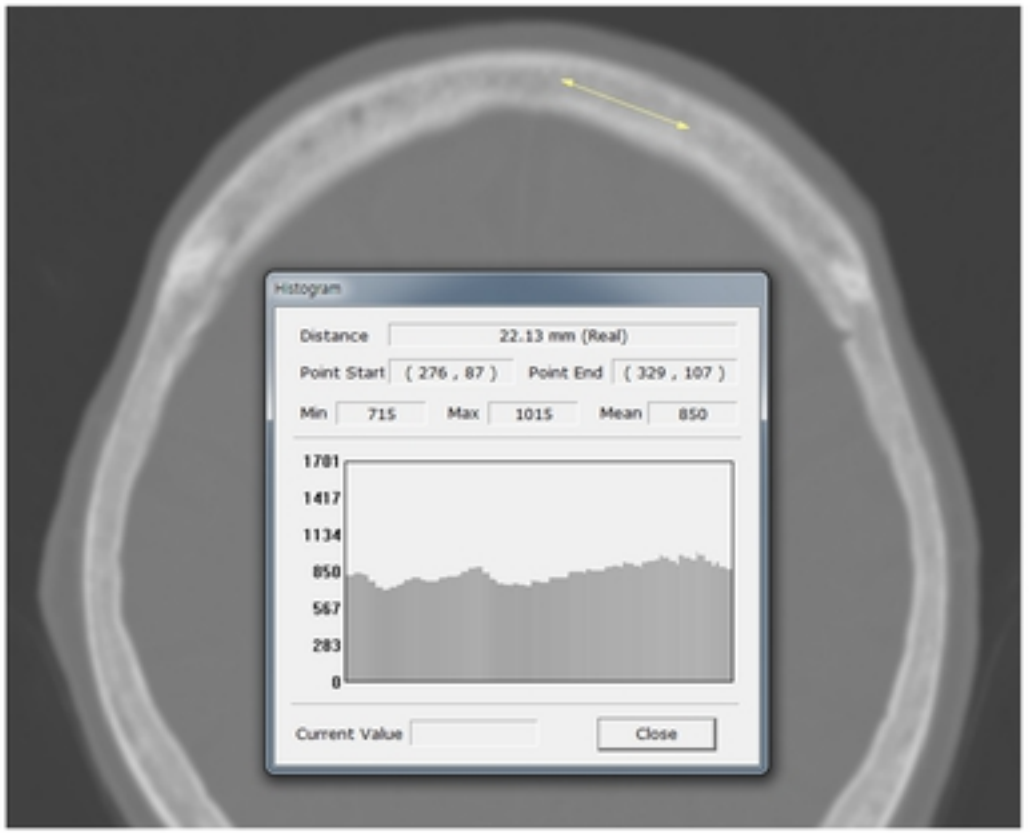

D

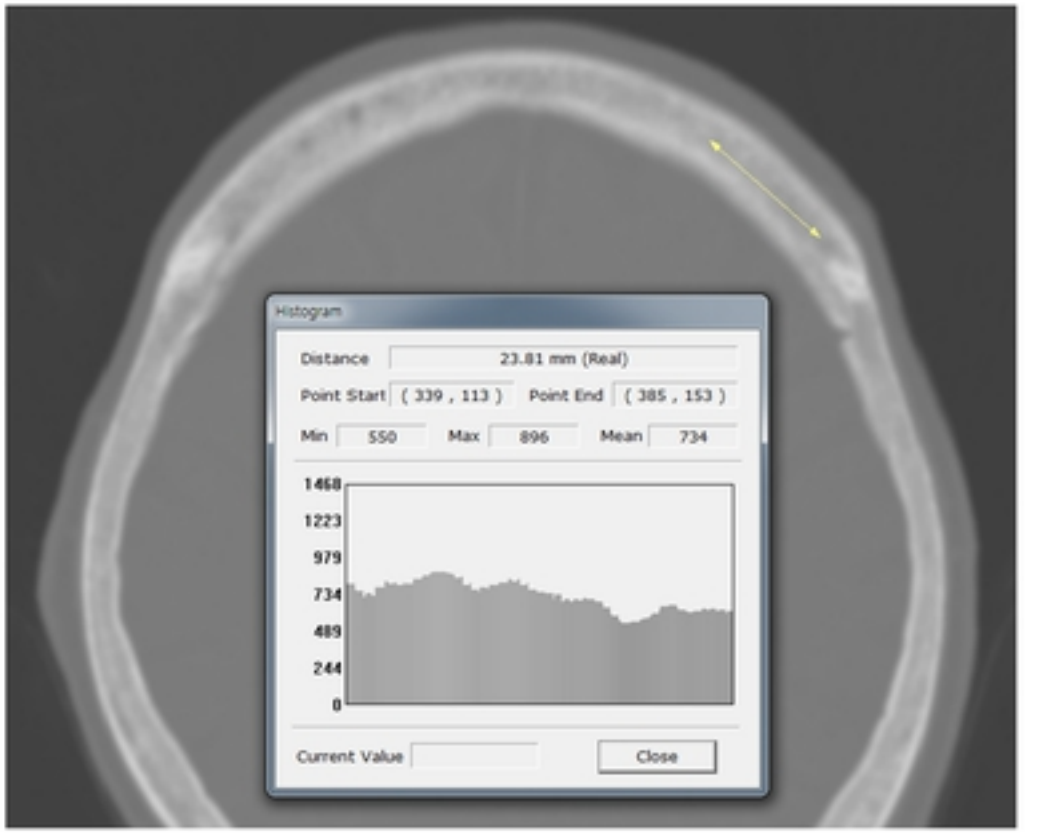

Figure1

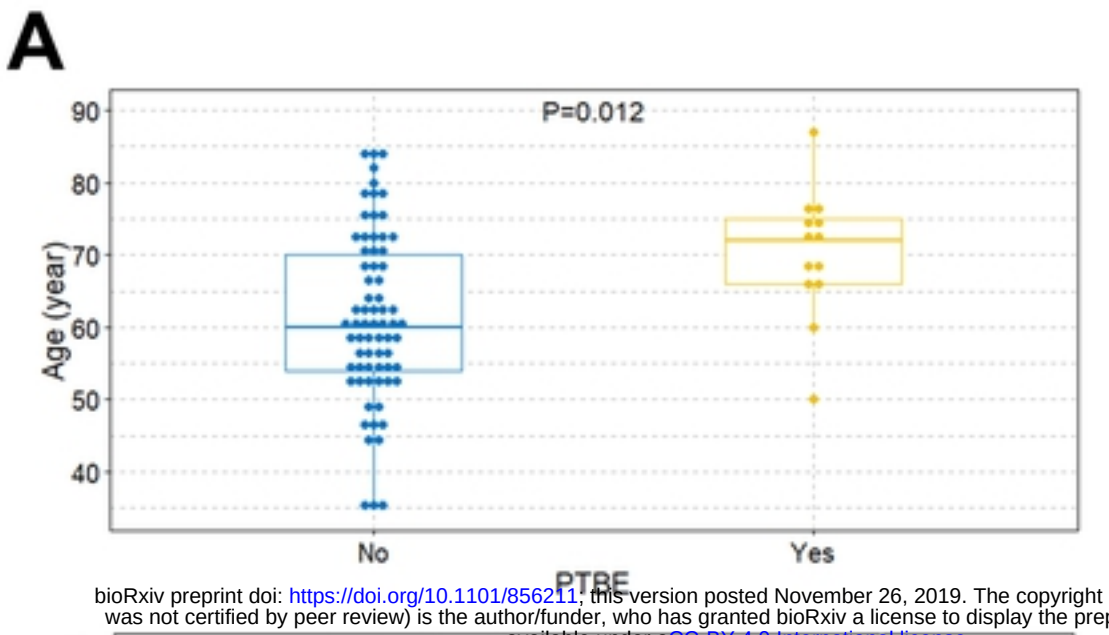

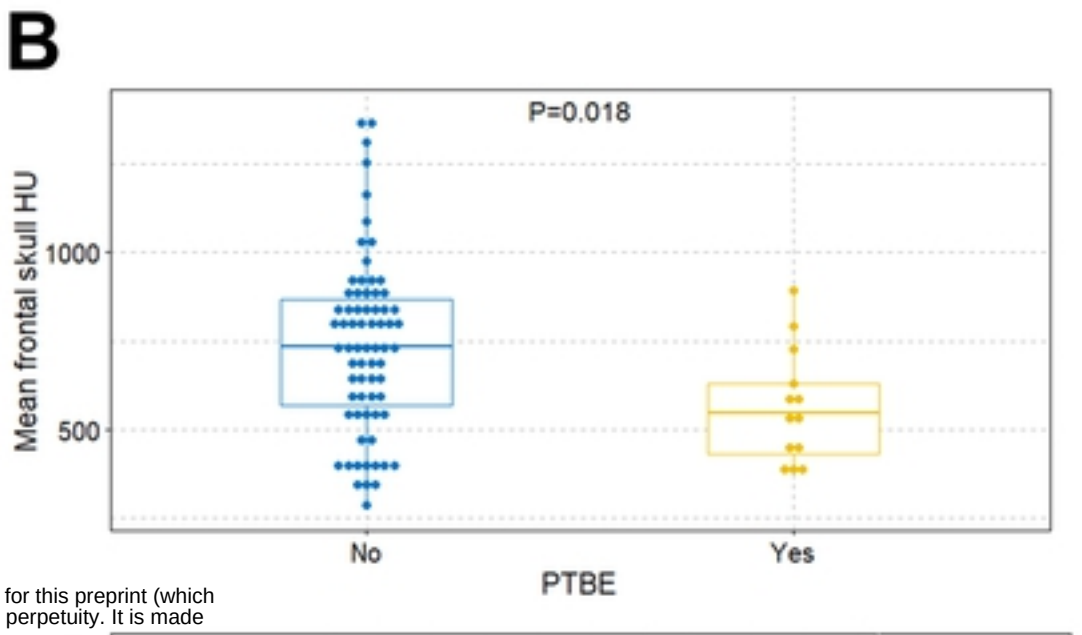

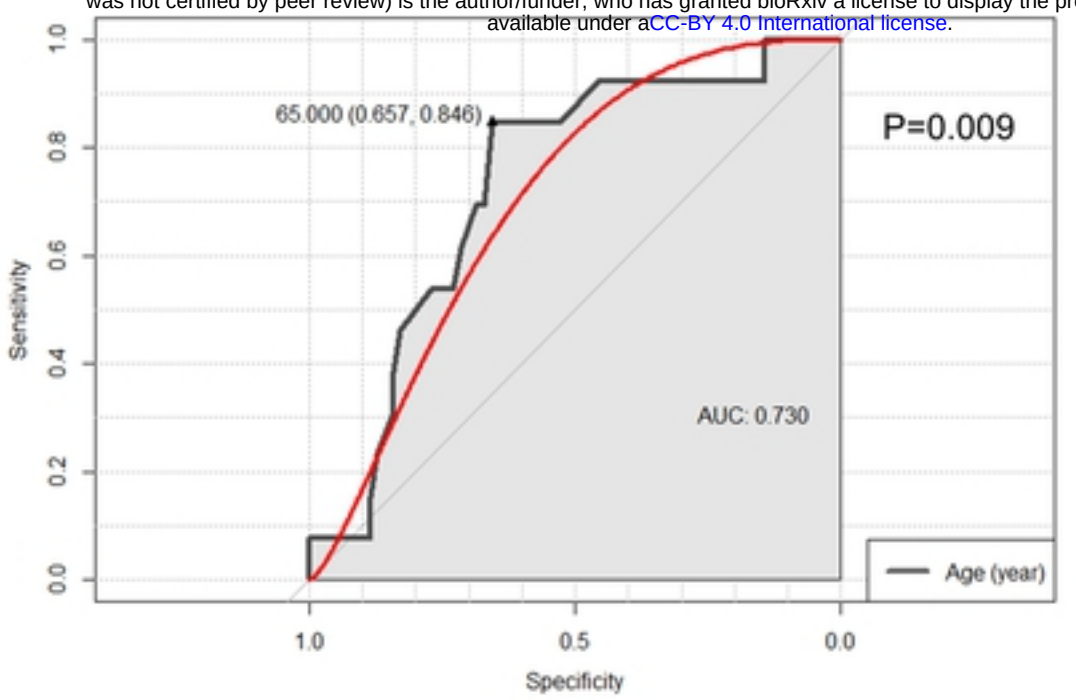

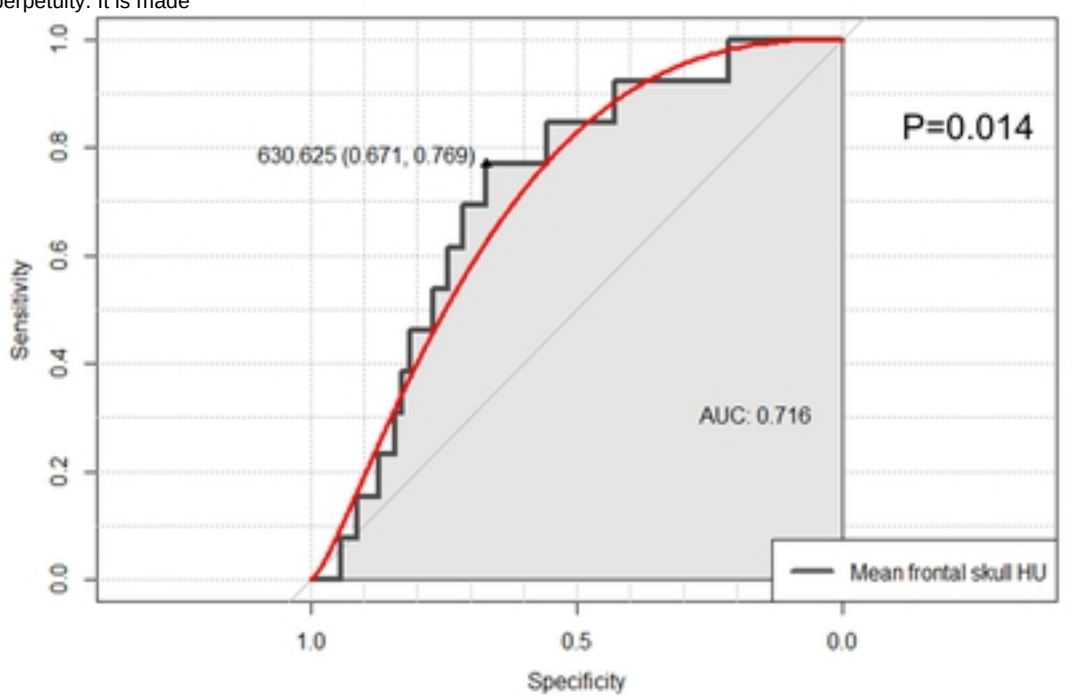

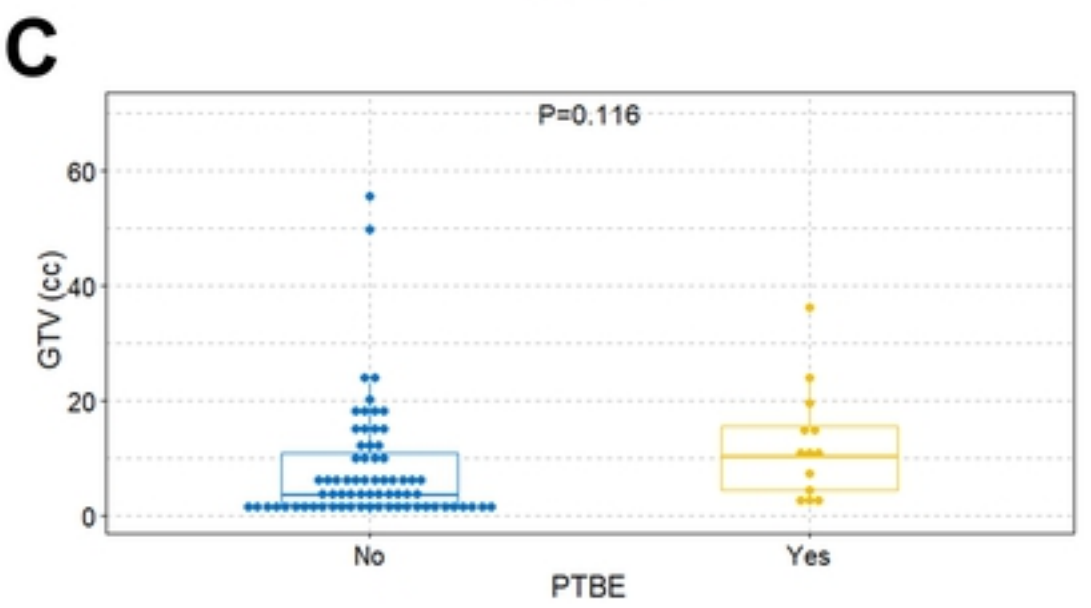

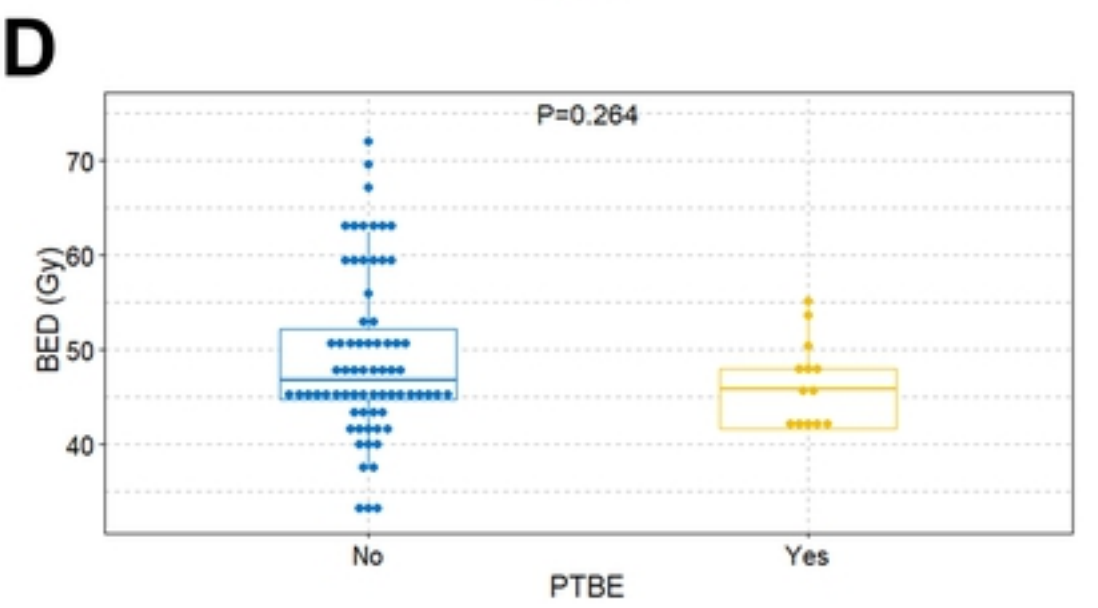

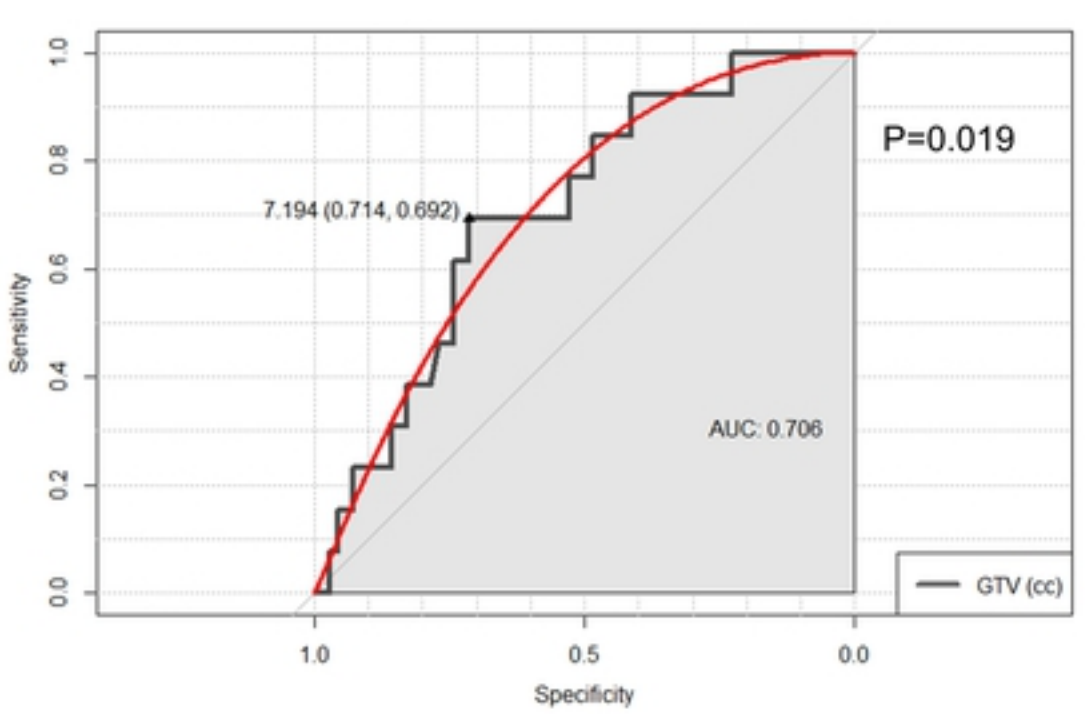

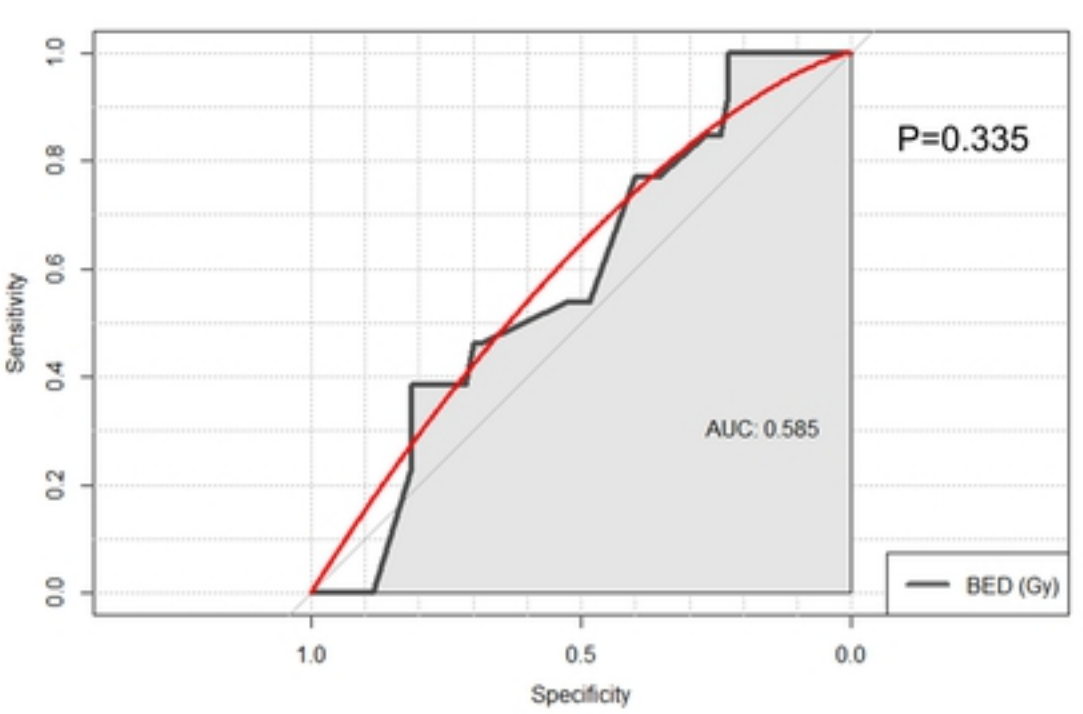

Figure2

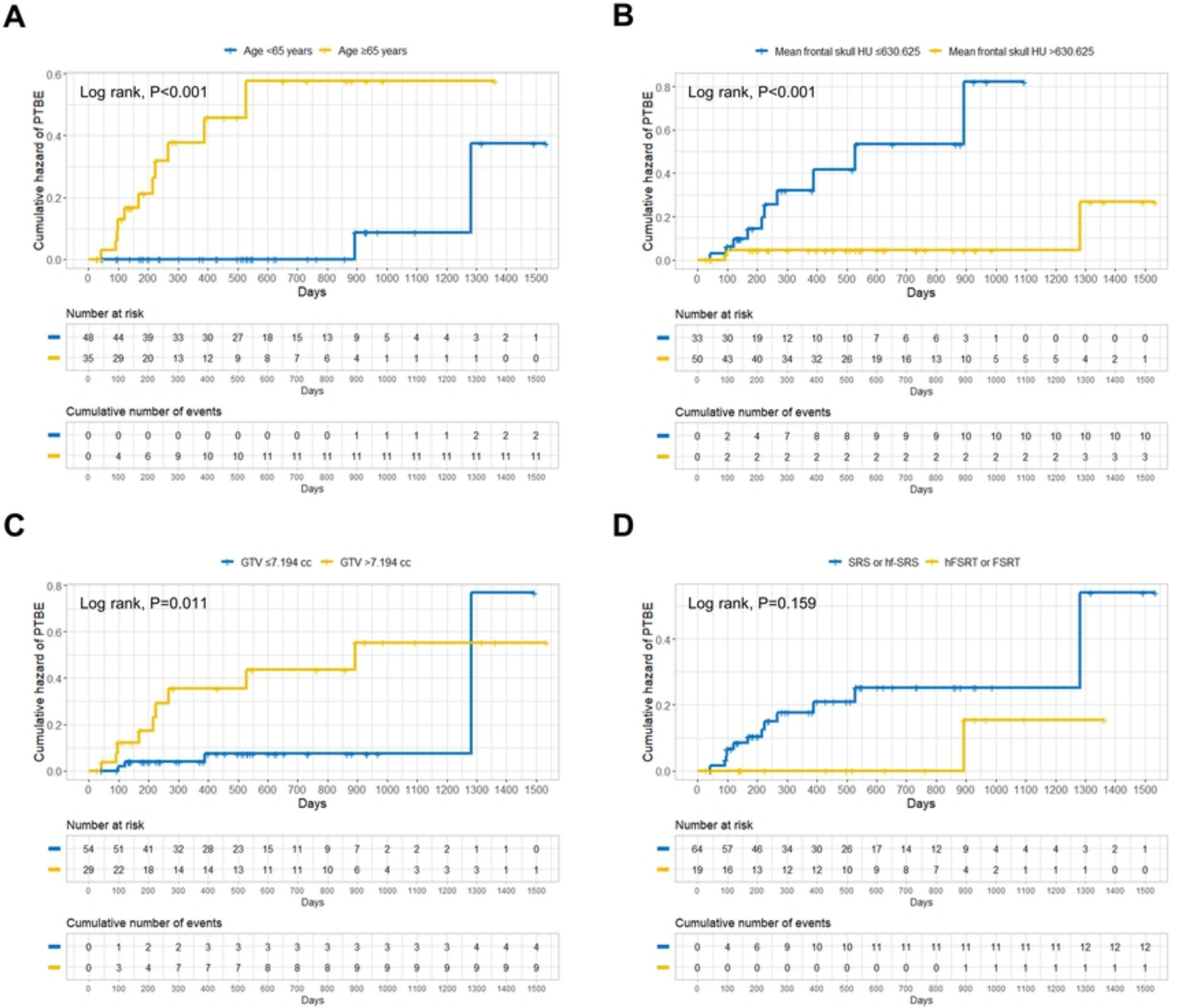

Figure3

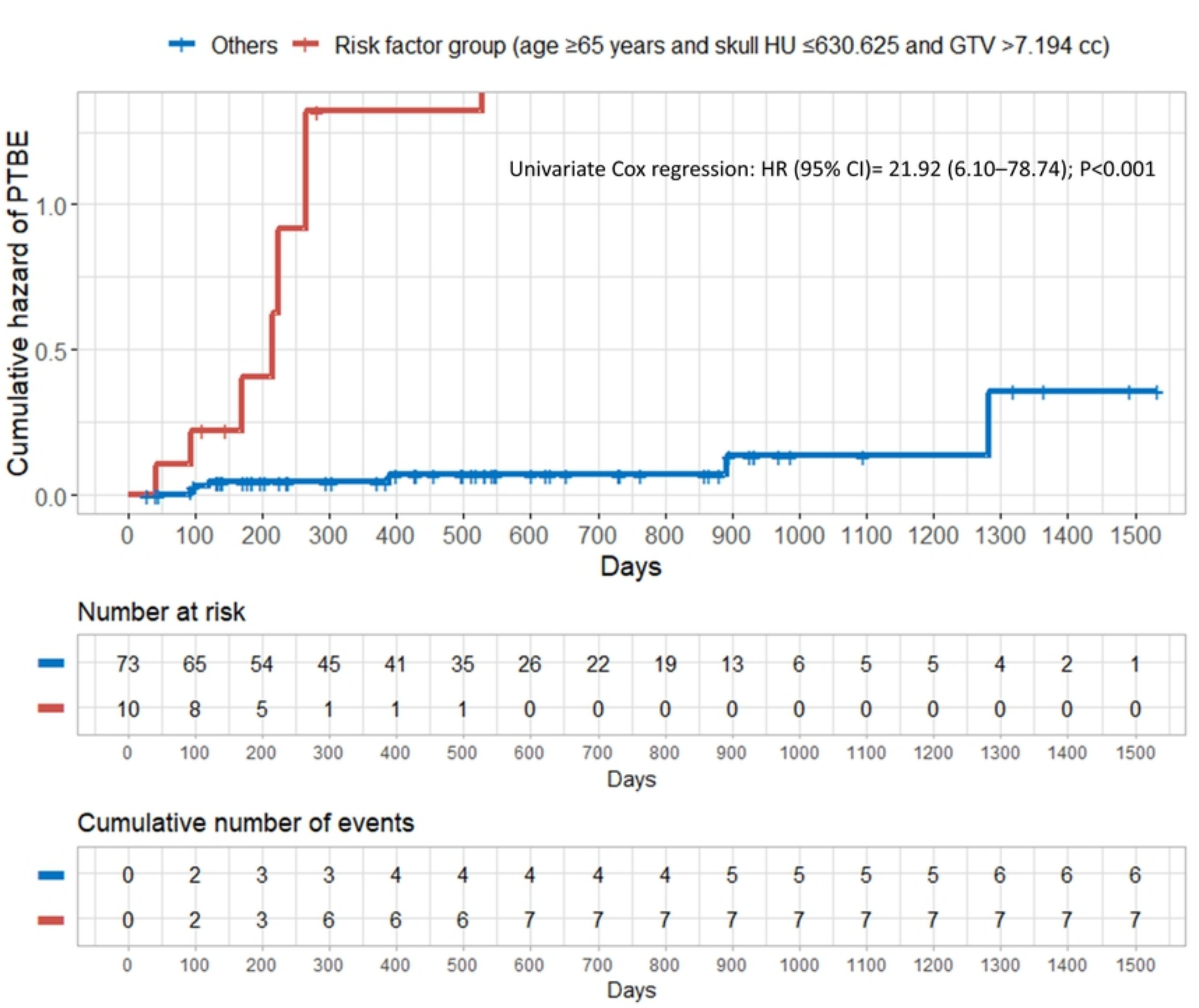
Others
Risk factor group (age ≥65 years and skull HU ≤630.625 and GTV >7.194 cc)
Univariate Cox regression: HR (95% CI)= 21.92 (6.10–78.74); P<0.001
Cumulative hazard of PTBE
1.0
0.5
0.0
0 100 200 300 400 500 600 700 800 900 1000 1100 1200 1300 1400 1500
Days
Number at risk
73 65 54 45 41 35 26 22 19 13 6 5 5 4 2 1
10 8 5 1 1 1 0 0 0 0 0 0 0 0 0 0
0 100 200 300 400 500 600 700 800 900 1000 1100 1200 1300 1400 1500
Days
Cumulative number of events
0 2 3 3 4 4 4 4 4 5 5 5 5 6 6 6
0 2 3 6 6 6 7 7 7 7 7 7 7 7 7 7
0 100 200 300 400 500 600 700 800 900 1000 1100 1200 1300 1400 1500
Days

Figure4